Biomedicine & Pharmacotherapy 133 (2021) 110936

Contents lists available at ScienceDirect

Biomedicine & Pharmacotherapy

journal homepage: www.elsevier.com/locate/biopha

Original article

Enhanced antitumor efficacy of lapachol-loaded nanoemulsion in breast cancer tumor model

Sued Eustáquio Mendes Miranda [a,b], Janaína de Alcântara Lemos [b], Renata Salgado Fernandes [b], Juliana de Oliveira Silva [b], Flaviano M. Ottoni [b], Danyelle M. Townsend [d], Domenico Rubello [c], Ricardo José Alves [b], Geovanni Dantas Cassali [e], Lucas Antônio Miranda Ferreira [b], Andre Luis Branco de Barros [a,*]

[a] Department of Clinical and Toxicological Analysis, Faculty of Pharmacy, Universidade Federal de Minas Gerais, 31270-901 Belo Horizonte, Minas Gerais, Brazil
[b] Department of Pharmaceutical Products, Faculty of Pharmacy, Universidade Federal de Minas Gerais, 31270-901 Belo Horizonte, Minas Gerais, Brazil
[c] Department of Nuclear Medicine, Santa Maria della Misericordia Hospital, Rovigo, Italy
[d] Department of Drug Discovery and Pharmaceutical Sciences, Medical University of South Carolina, USA
[e] Department of General Pathology, Institute of Biological Sciences, Universidade Federal de Minas Gerais, Belo Horizonte, MG, Brazil

ARTICLE INFO

Keywords:
Lapachol
Nanoemulsion
Antitumor activity
Breast cancer
Radiolabeling

ABSTRACT

Lapachol (LAP) is a natural compound with various biological properties, including anticancer activity. However, its clinical application is limited due to the low aqueous solubility and potential adverse side effects. Nanoemulsions are drug delivery systems that can assist in the administration of hydrophobic drugs, increasing their bioavailability and protecting from degradation. Thus, this study aimed to prepare a LAP-loaded nanoemulsion (NE-LAP), and evaluate its antitumor activity. For this purpose, the nanoemulsion was prepared using a hot homogenization method and characterized morphologically by cryogenic transmission electron microscopy (cryo-TEM). Mean diameter, polydispersity index, and zeta potential was evaluated by DLS, encapsulation efficiency was measured by HPLC. Moreover, the short-term storage stability, the drug release and hemolysis *in vitro* was determined. Additionally, pharmacokinetic, toxicology and toxicity properties of ^{99m}Tc-NE-LAP were evaluated in a breast cancer (4T1) tumor model. The cryo-TEM showed spherical globules, and the physicochemical characterization of NE-LAP showed a homogeneous stable nanoemulsion with a mean diameter of ~170 nm, zeta potential of around −20 mV, and encapsulation greater than 85 %. *In vitro* studies validated that encapsulation did not impair the cytotoxicity activity of LAP. The nanoemulsion was successfully radiolabeled and ^{99m}Tc-NE-LAP showed prolonged blood circulation and tumor affinity was confirmed by tumor-to-muscle ratio. Moreover, NE-LAP showed higher antitumor activity than the free drug and the treatment did not result in any signs of toxicity. Therefore, these findings suggest that NE-LAP can be considered an effective strategy for cancer treatment.

1. Introduction

Cancer is the second leading cause of death worldwide, behind only cardiovascular diseases [1]. Breast cancer is the most common tumor in women, with an incidence of 11.6 % and a mortality rate of 6.6 % [2]. Although chemotherapy is used as one of the main strategies for breast cancer treatment, several drawbacks including, multidrug resistance, adverse side effects, and low tumor cell specificity, often result in poor treatment efficacy [3,4]. Therefore, many approaches have been explored in an attempt to overcome these disadvantages. Strategies includes developing novel tumor-specific bioactive compounds or designing drug delivery systems to improve properties of FDA approved drugs with known biological activity [5,6].

Lapachol (LAP), a natural compound of the class of naphthoquinones, has several biological activities described, among them: antibacterial, trypanomicide, leishmanicide, and antitumor. LAP has been tested *in vitro* against several cancer cell lines and *in vivo* in some animal models [7,8]. However, the occurrence of adverse side effects, such as anemia, nausea, and vomiting, along with its poor water solubility and low bioavailability have limited the clinical use of this drug

* Corresponding author.
E-mail address: albb@ufmg.br (A.L.B. de Barros).

https://doi.org/10.1016/j.biopha.2020.110936
Received 30 July 2020; Received in revised form 21 October 2020; Accepted 23 October 2020
Available online 27 November 2020

[9].

Nanometer-scale drug delivery systems are promising alternatives to increase the antitumor efficacy of drugs and to reduce their adverse side effects [10]. Nanoemulsion is a dispersion of two immiscible liquids, typically water and oil, on a nanometer scale (20−200 nm), stabilized by surfactants [11–13]. It is an attractive delivery platform since it can encapsulate hydrophobic drugs, allowing high payloads in a low concentration of oil [14]. The use of nanoemulsions have shown favorable data in drug stability, cellular uptake, and blood circulation time, in both *in vitro* and *in vivo* tumor models [15–18]. Regarding LAP, some studies reported the encapsulation of the drug as a strategy to overcome its limitations, nevertheless, none of them are used for intravenous application or antitumor evaluation [19–23]. Thus, this study aimed to evaluate the antitumor activity of nanoemulsion loaded with LAP (NE-LAP). To achieve this purpose, the system was characterized as the mean diameter, polydispersity index, zeta potential, encapsulation efficiency, and drug release. In addition, NE-LAP was radiolabeled with technetium-99 m for evaluating the ability of the system to reach the tumor site. Moreover, the antitumor efficacy and toxicity was evaluated in 4T1 breast tumor model in BALB/c mice.

2. Material and methods

Ethoxylated sorbitan monooleate (SuperRefined™Polysorbate™ 80; Tween 80™), soybean oil, glycerol, lapachol, and $SnCl_2{\cdot}2H_2O$ were purchased from Sigma-Aldrich (Steinheim, Germany). RPMI 1640 Medium, fetal bovine serum, penicillin, streptomycin, and trypsin EDTA 0.25 % were purchased from Gibco-Invitrogen (Waltham, MA, USA). ^{99m}Tc was obtained from an alumina-based $^{99}Mo/^{99m}Tc$ generator (IPEN, São Paulo, Brazil). Xylazine solution (Dopaser® 2 %) was purchased from Hertape Calier (Juatuba, Brazil). Ketamine hydrochloride solution (Dopalen® 10 %) was supplied by Vetbrands Agroline (Campo Grande, Brazil). All other chemicals were of analytical grade. The subcutaneous tumor model was established in 8-week female BALB/c mice purchased from CEBIO-UFMG (Belo Horizonte, Brazil). All animal studies were approved by the Institutional Animal Care and Use Committee (CEUA/UFMG) under protocol # 06/2018.

2.1. Nanoemulsion preparation

Oil-in-water (O/W) nanoemulsions (NE) were prepared using the hot homogenization method. The composition of the nanoemulsion in the oily phase (Soybean oil, 400 mg; Polysorbate 80, 115 mg), and the aqueous phase (Glycerol, 224 mg; ultrapure water, 10 mL) were heated, separately, to 80 °C. With the temperature maintained at 80 °C, aqueous phase was gently dropped onto the oily phase under constant agitation, at 8000 rpm, with an Ultra Turrax T-25 homogenizer (Ika Labortechnik, Germany). The formed emulsion was immediately submitted to a high-intensity probe sonication for 10 min (CPX 500 model, Cole-Palmer Instruments, USA). After this period, the formulations were cooled down to room temperature with manual agitation and the volume was adjusted to 10 mL with ultrapure water. The pH of the NE was adjusted to 7.0 with a solution of NaOH (0.1 mol L^{-1}) and the formulations were stored at 4 °C. For NE-LAP, the drug was added to the oily phase at different concentrations (0.05 %; 0.075 %; 0.1 %) and the same method of preparation was used.

2.2. Particle size, polydispersity index (PDI), Zeta potential

The mean particle diameter and PDI were measured by dynamic light scattering (DLS) using a Zetasizer Nano ZS90 (Malvern Instruments, UK). Zeta potential measurements were carried out by DLS associated with electrophoretic mobility. The samples were diluted 100-times in ultrapure water.

2.3. Encapsulation efficiency (EE)

NE-LAP was purified by 0.45 μm filtration. By using this strategy, encapsulated LAP freely pass through the membrane while non-encapsulated LAP remains in the filter. For EE quantification, samples of total LAP (before filtration) and purified LAP (after 0.45 μm filtration) were dispersed in THF:Methanol (4:6) mixture and the drug concentration was determined by HPLC (Waters, 515 isocratic pump, 717 plus automatic injector, and UV-Dual λ 2487 detector, Milford, EUA) using methanol: 5 % acetic acid (80:20 (v/v)) as mobile phase, Innoval reversed-phase C_{18} column, (5 μm, 4.6 × 150 mm) (Agela Technologies, Tianjin, China); flow 1.0 mL/min; 25 °C, 20 μL injection volume and column oven at 40 °C, with UV detection in λ = 278 nm [24]. Then, the %EE was calculated by the formula:

$$\%EE = \frac{E_{LAP} \times 100}{T_{LAP}}$$

Where: T_{LAP} = total LAP concentration in NE, E_{LAP} = Encapsulated LAP concentration.

2.4. Morphological analysis

Transmission electron cryo-microscopy (cryo-TEM) (Tecnai G2-12 - FEI SpiritBiotwin 120 kV) were used to study the morphology of NE-LAP. The samples were prepared by plunge freezing technique, by spreading the sample into a thin film across an EM grid and then rapidly submerging it in liquid ethane. Mean diameter was determinated by the analyses of 100 nanoparticles, using Image J software.

2.5. Short-term storage stability

Immediately after preparation, NE-LAP at concentrations of 0.5, 0.75, and 1.0 mg/mL were stored at 4 °C, protected from the light. At 3, 7, 15, and 30 days post-preparation NE-LAP were evaluated as mean diameter, zeta potential, and encapsulation efficiency.

2.6. Colloidal stability

The stability of the NE-LAP was investigated in different biological fluids to predict the *in vivo* behavior of the drug delivery system. NE-LAP was diluted 4-times in NaCl (0.9 % w/v), PBS buffer (pH 7.4), Dulbecco Modified Eagle Medium (DMEM) or murine plasm. The resulting solution was kept at 37 °C under agitation of 150 RPM, for 24 h [25]. At pre-determined time points aliquots of each solution were collected and mean diameter was measure by DLS.

2.7. Polarized light microscopy (PLM)

The presence of LAP crystals in the nanoemulsion dispersion was evaluated by an optical microscope (Zeiss Axio Imager.M2, Carl Zeiss, Germany) coupled with polarized light and equipped with an AxioCam digital camera (Model ERc 5S, Carl Zeiss, Germany). The samples were prepared in microscope slides (undiluted). The detection of LAP crystal indicates the presence of non-encapsulated LAP, and therefore, lack of stability.

2.8. In vitro drug release

The release of LAP from NE was performed by the dialysis method using tubing cellulose membranes with a cutoff size of 14 kDa and a diameter of 21 mm (cellulose ester membrane; Sigma–Aldrich, St Louis, USA). Dialysis bags were filled with 1 mL of formulation, sealed and incubated with 50 mL of PBS (pH 7.4) containing Tween 80 (2 %), at 37 °C, for 24 h, under magnetic stirring at 150 rpm. An aqueous solution of LAP (in PBS containing 2 % Tween 80) was used as a control (concentration 0.46 mg/mL). At 15, 30, 60, 90, 120, 240, 360, and 1440 min,

aliquots were withdrawn and LAP concentration was analyzed by HPLC. The same volume was replaced with the receptor liquid (PBS + Tween 80). Values were plotted as cumulative percentage of drug release.

2.9. Radiolabeling of NE-LAP

Radiolabeling of NE-LAP was carried out in a sealed vial containing 1.0 mL NE-LAP and 100 μL $SnCl_2{\cdot}H_2O$ solution in 0.25 mol L^{-1}HCl (1.0 mg/mL). The pH was adjusted to 7.4 using NaOH (1 mol L^{-1}), and vacuum was performed to the vial. An aliquot of 0.1 mL of $Na^{99m}TcO_4$ (3.7 MBq) was added to the vial and maintained at room temperature for 15 min.

Radiolabeling yield was determined by thin-layer chromatography (TLC-SG, Merck, Darmstadt, Germany) using acetone as the mobile phase to quantify $^{99m}TcO_4^-$. Radioactivity was determined using a gamma counter (Wallac Wizard 1470-020 Gamma Counter, PerkinElmer Inc., Waltham, Massachusetts, USA). $^{99m}TcO_2$ was removed from the preparation using a 0.45 μm syringe filter [26].

2.10. In vitro radiolabeling stability

The radiolabeling stability of ^{99m}Tc-NE-LAP at room temperature in 0.9 % (w/v) NaCl and in the presence of mouse plasma to simulate *in vivo* conditions were performed. Briefly, a volume of 90 μL of ^{99m}Tc-NE-LAP was incubated, under agitation, at 37 °C (Dubnoff Bath MA-095/CF) with 1.0 mL of fresh mouse plasma. Radiolabeling stability was determined by TLC-SG from samples taken at 1, 2, 4, 8, and 24 h after incubation, according as previously described [27].

2.11. Blood clearance

The blood clearance was performed according to published procedures [27]. Aliquots of 3.7 MBq of ^{99m}Tc-NE-LAP were injected intravenously into healthy BALB/c mice. An incision was made in the tail of the animals and blood was collected in pre-weighed tubes at times of 1, 5, 10, 15, 30, 45, 60, 90, 120, 240, 480, and 1440 min after administration. The tubes were weighed and their radioactivity determined by a gamma counter. These data were used to plot a percentage of the dose injected per gram of blood (% ID/g) *versus* time.

2.12. Cell culture

The breast cancer cell line (4T1) was grown in RPMI 1640 medium, supplemented with 10 % (v/v) of fetal bovine serum, penicillin (100 IU/mL), and streptomycin (100 μg/mL). Cells were maintained in in 5 % CO_2 at 37 °C. The cells were grown to confluence and harvested by trypsinization.

2.13. Tumor cell inoculation

Aliquots of 1.0×10^6 4T1 cells in RPMI medium (0.1 mL) was injected (SC) into the right flank of female BALB/c mice. Mice were kept in an area with light control, with free access to water and food. Tumor cells were allowed to grow *in vivo* for 7 days, once the tumor volume reached about 100 mm^3.

2.14. Tumor-to-muscle ratio

Aliquots of 3.7 MBq of ^{99m}Tc-NE-LAP were injected intravenously into tumor-bearing BALB/c mice. At 1, 4, 8, and 24 h post-injection, the tumor and surrounding muscle were removed, dried on filter paper, and weighed. The radioactivity in each tissue was determined by a gamma counter. A standard dose containing the same injected amount was counted simultaneously in a separate tube, which was defined as 100 % radioactivity. The results were expressed as the tumor-to-muscle ratio in order to assess the tumor affinity of the ^{99m}Tc-NE-LAP.

2.15. Cell viability

MDA-MB-231 and 4T1 cells were seeded in 96-well plates (1×10^4 cells/well and 5×10^3cells/well, respectively) 24 h prior to treatment. Cells were exposed to a series of concentrations of buffered solution of LAP, NE-LAP, and blank NE, for 48 h. Cell viability was assessed using the sulforhodamine B (SRB) assay as previously described [28]. Briefly, after incubation, 10 % trichloroacetic acid (TCA) was added to each well to fix cells for one hour. Plates were then washed with water to remove TCA and stained with SRB for 30 min. Afterward, the plate was washed with 1 % acetic acid to remove the unbound SRB. Then, the protein-bound dye was solubilized in 10 mM of Tris-Base [tris (hydroxymethyl) aminomethane] solution and optical densities (OD) were read at 510 nm on a microplate spectrophotometer Spectra Max Plus 384 (Molecular Devices, Sunnyvale, CA, USA).

2.16. Hemolysis assay

Fresh mice blood (8 weeks, 20.0 ± 2.0 g) was collected in tubes containing 10 % w/v EDTA solution. The red blood cells (RBC) were separated by centrifugation at 3000 rpm for 10 min at room temperature (Heraeus Multifuge X1R Centrifuge, Germany). The RBC collected from the bottom were washed with NaCl 0.9 % (w/v) until a colorless supernatant was obtained above the cell mass. The final pellet was diluted with NaCl 0.9 % (w/v) solution to obtain a 4 % (w/v) RBC concentration. NE-LAP of three different concentrations of LAP were evaluated. The samples were incubated with an equal volume of 4 % RBC suspension (n = 5) for 1 h at 37 °C under agitation at 500 bpm (metabolic bath, Dubno ff ; MA-95/CF Marconi, Brazil). After the incubation, the cell suspensions were centrifuged at 2000 rpm for 5 min and the absorbance of the supernatants was measured in a spectrophotometer (Evolution 201 UV–vis Spectrophotometer Thermo Scientific, USA) at 540 nm. Deionized water and NaCl 0.9 % (w/v) were used as negative and positive controls, respectively. The percent hemolysis was calculated for each sample by taking the absorbance of positive control as 100 % hemolytic sample, using following equation:

$$\text{Hemolysis (\%)} = [(\text{Absorbance sample})/(\text{Absorbance positive control})] \times 100$$

2.17. Antitumor activity

For the antitumor activity assay only the 4T1 tumor model was used. On the 7th day after 4T1 cell inoculation, once the tumor volume reached ~100 mm^3, the mice were randomly assigned into three groups (n = 7 for each group): group 1: PBS-Tween 80 at 2 % (negative control group); group 2: buffered solution of LAP; group 3: NE-LAP. For all treatments, the dose of LAP was 5 mg/kg, in a total of 5 administrations, every 2 days, injected by the tail vein. Throughout the study, tumors were measured with a caliper every 2 days. Tumor volumes were calculated from the formula:

$$V = (d_1)^2 \times d_2 \times 0.5$$

Where d_1 and d_2, represent the smaller and larger diameter, respectively [29].

At the end of the experimental period (D10), the relative tumor volume (RTV), and the tumor growth inhibition ratio (IR) were determined by the formulas:

$$RTV = \frac{\text{Tumor volume on day10}}{\text{Tumor volume on day 0}}$$

$$IR = \frac{\text{Mean RTV from each treatment} \times 100}{\text{Mean RTV from control group}}$$

At the end of the experiment, the animals were euthanized and the

Table 1
Particle size, PDI, zeta potential, entrapment efficiency (EE) and Drug concentration of NE- blank and NE-LAP at 3 different concentrations of LAP (0.5, 0.75, and 1.0 mg/mL).

	Size (nm)	PDI[a]	Zeta (mV)	EE (%)	Drug concentration (μg/mL)
NE	174 ± 14	0.201 ± 0.040	−26.0 ± 8.3	–	
NE-LAP 0.5	178 ± 6	0.175 ± 0.019	−20.6 ± 7.8	100.3 ± 1.5	501,6 ± 7,3
NE-LAP 0.75	174 ± 2	0.179 ± 0.020	−17.9 ± 4.0	97.3 ± 2.9	729,8 ± 21,8
NE-LAP 1.0	176 ± 6	0.170 ± 0.025	−21.9 ± 2.8	85.4 ± 3.7	853,9 ± 37,6

[a] Polydispersity index.

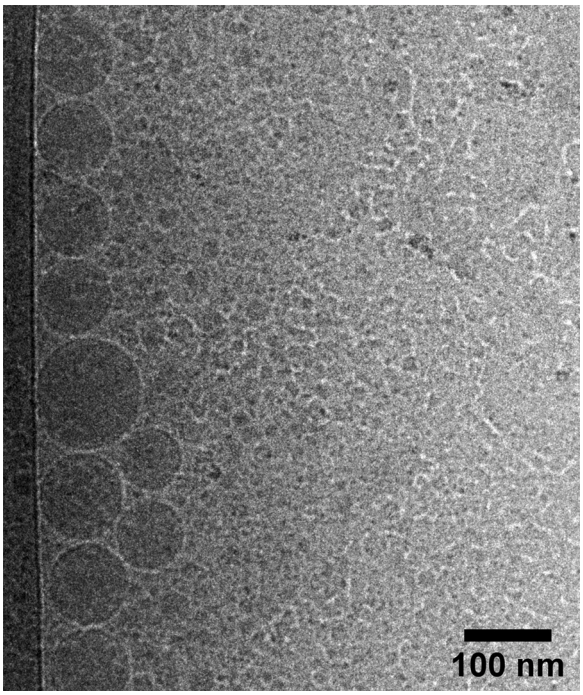

Fig. 1. Cryogenic Transmission Electron Microscopy of NE-LAP, 100 nm scale bar.

blood collected, in the presence of EDTA, for toxicity evaluation [29].

2.18. Histological analysis

The liver and kidney were collected for histopathological analysis. Samples were fixed in 10 % buffered formalin for 48 h, dehydrated in alcohol and included in paraffin blocks. 4 μm sections were obtained and stained with hematoxylin and eosin (H&E). The slides were evaluated by a trained pathologist and images were captured by a camera connected to an optical microscope (Olympus BX-40; Olympus, Tokyo, Japan).

2.19. Biochemical analysis

Blood was collected using EDTA as an anticoagulant and centrifuged at 5000 rpm for 10 min and plasma was obtained. Plasma was used to perform biochemical analyses such as urea, creatinine, AST (aspartate aminotransferase), and ALT (alanine aminotransferase). The biochemical tests were performed using commercial kits from Labtest® (Lagoa Santa, Brazil) through Bioplus BIO-2000 semiautomatic analyzer equipment (São Paulo, Brazil).

2.20. Statistical analysis

Data are expressed as mean ± SD. Statistical analyses were performed using GraphPad PRISM, version 5.00 software (GraphPad Software Inc., La Jolla, CA, USA). The difference between the experimental groups was tested using one-way analysis of variance (ANOVA), followed by the Tukey test, or T test, when the number of groups evaluated was equal to two. All data showed normal distribution and homoscedasticity, when necessary. The differences were considered statistically significant when the P values were <0.05.

3. Results

3.1. Characterization

Blank NE and NE-LAP at different concentrations of LAP, were characterized as mean diameter, PDI, zeta potential, %EE, and the results are summarized in Table 1. All blank and LAP formulations showed a mean diameter of ~ 175 nm, with low polydispersity index values ($\leq$ 0.2), indicating monodisperse size distribution. These values are in agreement with what is recommend for intravenous administration [30]. Particles with sizes between 100 and 200 nm are favorable for intravenous administration, as they are large enough to prevent absorption in the liver and small enough to avoid filtration in the spleen [30,31]. Moreover, nanosystems with a size smaller than 200 nm are advantageous since they may reduce opsonization and consequently the uptake by the cells of the mononuclear phagocytic system [32,33].

The highly negative zeta potential is a good indication of stability since high values, in module, may inhibit droplet fusion by charge repulsion. Encapsulation content was high to all formulations, as expected in nanoemulsion systems, due to the hydrophobic nature of LAP. The encapsulation value decreased as the drug concentration increased, suggesting saturation of the system [34–36].

Representative cryo-TEM image is shown in Fig. 1. Images showed good sample preparation and dispersion. It can be observed nanoparticles as round globules, with smooth surface and, an average size of approximately 165 nm, which is consistent with DLS data.

3.2. Short-term storage stability

NE-LAP at different concentrations of LAP were prepared and stored at 4 °C. The storage stability over time was evaluated as demonstrated in Fig. 2.

As observed in Fig. 2A and B, the mean diameter and PDI did not change over time indicating the stability of the NE-LAP up to 30 days. Importantly, the average size of particles remains in the range of 200 nm, which is compatible with intravenous administration, and PDI showed values always lower than 0.3 indicating particles homogeneously distributed [31]. Moreover, a negative zeta potential value (~20 mV) was achieved throughout the whole experiment (Fig. 2C).

The encapsulation stability was also evaluated within 30 days and results are shown in Fig. 2D. NE-LAP at concentrations of 0.75 mg/mL and 1.0 mg/mL showed low stability over time, resulting in significant drug release after 7 and 3 days, respectively. Both NE-LAP released more than 50 % of the drug at the end of the experiment. NE-LAP at 0.5 mg/mL showed excellent stability within 30 days of storage.

Stability was assessed by polarized light microscopy. Fig. 3 shows a representative image on the day of the instability of each formulation or day 30 if no instability was observed. Therefore, crystals were present for NE-LAP at 1.0 mg/mL at day 3 (Fig. 3A) and for NE-LAP at 0.75 mg/

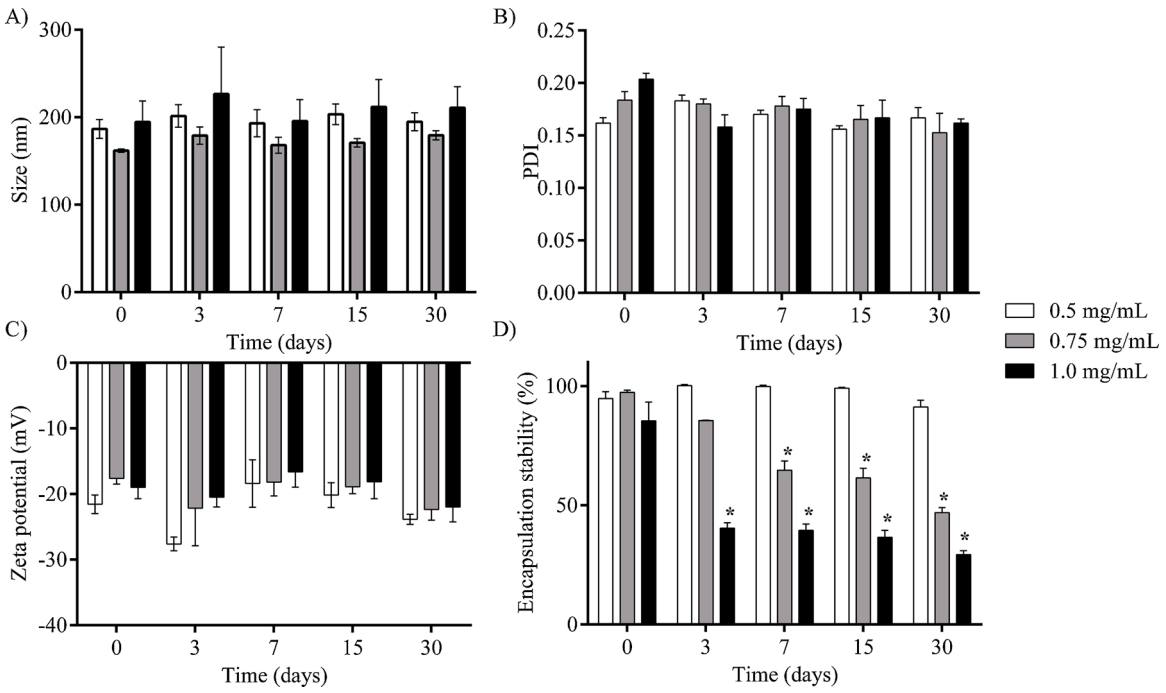

Fig. 2. Storage stability of NE-LAP at different concentrations of LAP stored at 4 °C, for 30 days. A) Mean diameter, B) PDI, C) zeta potential, D) Encapsulation Stability. (* Represents statistical diff ;erences ($P < 0.05$) compared to day 0).

Fig. 3. Polarized light microscopy images of NE-LAP at different concentrations. Images were taken on the day of the instability of each formulation or day 30 if no instability was observed. A) NE-LAP, 1.0 mg/mL, at day 3; B) NE-LAP, 0.75 mg/mL, at day 7; C) NE-LAP, 0.5 mg/mL, at day 30. 5X magnification.

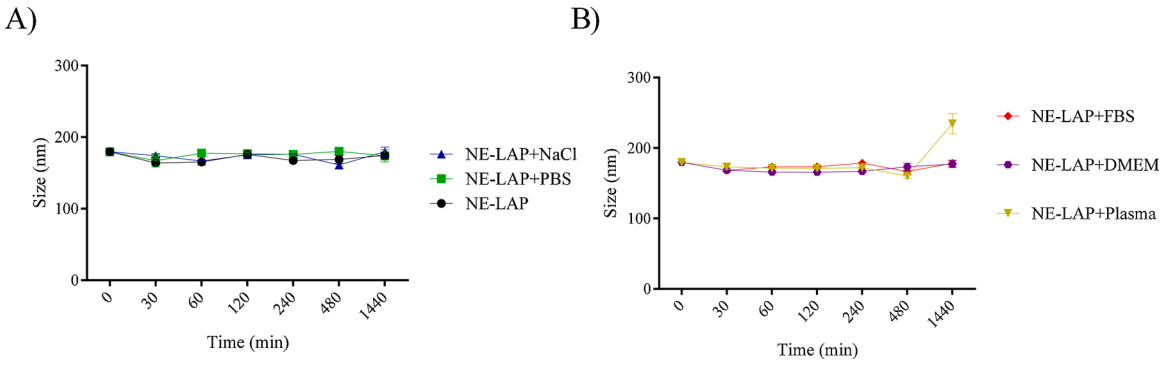

Fig. 4. Colloidal stability assay in several biological fluids, NE-LAP were diluted three times. A) NE-LAP; NE-LAP in NaCl (0.9 %); NE-LAP in phosphate-saline buffer (PBS). B) NE-LAP in Fetal Bovine Serum (FBS); NE-LAP in Dulbecco Modified Eagle Medium (DMEM); NE-LAP in murine plasma.

mL at day 7 (Fig. 3B). In contrast, no crystals were observed in NE-LAP at 0.5 mg/mL even after 30 days of storage (Fig. 3C). Altogether, the stability studies indicate that 0.5 mg/mL is the optimum concentration for achieving a more stable nanoemulsion. Therefore, NE-LAP at 0.5 mg/mL was used for further *in vitro* and *in vivo* assays.

3.3. Colloidal stability

The colloidal stability of the NE-LAP was investigated in diff ;erent media, such as NaCl (0.9 % w/v), PBS, DMEM, mice plasma. The evaluated parameters are summarized in Fig. 4. It was found that NE-LAP showed excellent stability, independently of the media, without any significant change in the particle mean diameter in 24 h.

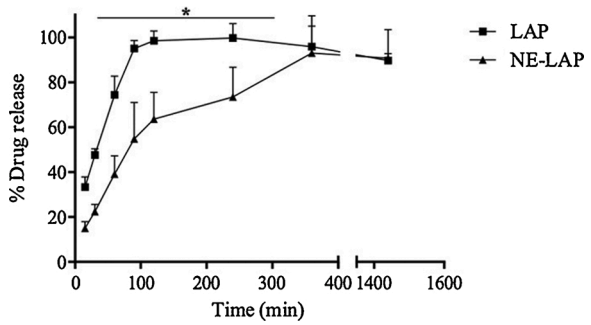

Fig. 5. *In vitro drug* release profile of LAP from nanoemulsion (NE-LAP) at 37 °C for 24 h (* Represents statistical differences ($P < 0.05$) between LAP and NE-LAP).

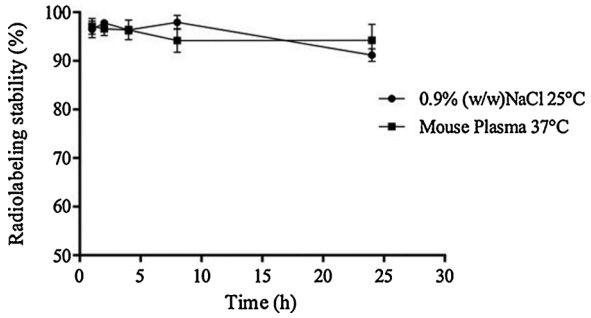

Fig. 6. Radiolabeling stability of ^{99m}Tc-NE-LAP in the presence of 0.9 % (w/v) NaCl, at 25 °C or mouse plasma, at 37 °C, as a function of time (n = 7).

3.4. In vitro drug release

Fig. 5 shows the release profile of free and encapsulated LAP. Here we showed that the free LAP reached 100 % release within approximately 1.5 h. In contrast, NE-LAP at 0.5 mg/mL showed a more sustained release, reaching 100 % after six hours. Nanoemulsions are characterized by a gradual release of the drug, and other authors have shown controlled release of the drug from nanoemulsion in a similar manner [37].

3.5. Radiolabeling yield and stability

Following radiolabeling, impurities were quantified. The radiolabeling yield of ^{99m}Tc-NE-LAP was 94.5 ± 1.3 %, which is superior to that recommended by the American Pharmacopoeia [38]. The results of radiolabeling stability are presented in Fig. 6. ^{99m}Tc-NE-LAP was highly stable up to 24 h with than 90 % of the radiometal remaining in the nanoparticles. This finding is extremely important to guarantee that animal studies data will reflect the nanoparticles' fate instead of the ^{99m}Tc itself [27].

3.6. Blood clearance and tumor-to-muscle ratio

Pharmacokinetic properties were evaluated in tumor bearing mice. Blood clearance for ^{99m}Tc-NE-LAP is shown in Fig. 7A. ^{99m}Tc-NE-LAP decays in a biphasic manner showing a α-half-life of 3.8 min and a β-half-life of 117.3 min. The area under the curve (AUC) was 2918 %ID.min^{-1}.

It is important to underscore that ^{99m}Tc-NE-LAP showed better parameters when compared with previous studies of ^{99m}Tc-LAP reported by our group [27]. There was a large increase in the β-half-life from 50 to 117.3 min and a considerable increment in the AUC from 1909 to 2918 % ID.min^{-1} [27]. These results clearly showed the contribution of the nanoemulsion in prolonging blood circulation time of the drug, which is of pivotal importance to enhance tumor accumulation and consequently a high antitumor efficacy.

A biodistribution study was performed in order to evaluate specific tumor uptake of ^{99m}Tc-NE-LAP. Fig. 7B shows the tumor-to-muscle ratio, which is an important parameter to identify the tumor affinity compared with the surrounding tissue. Tumor-to-muscle ratio increases over time reaching the maximum after 24 h (6.49). These data indicate that the ^{99m}Tc-NE-LAP accumulates preferentially in the tumor than the surrounding muscle. It is important mentioning that the tumor-to-muscle ratio for ^{99m}Tc-NE-LAP was higher than that previously reported for ^{99m}Tc-LAP [27]. The preferential tumor accumulation of NE-LAP is a relevant parameter to guarantee the proper access to the target tissue in a tumor treatment protocol.

3.7. Cell viability

Cell viability was assessed using the sulforhodamine B (SRB) assay against a human and a murine breast cancer cell line, 4T1 and MDA-MB-231, respectively. Half-maximum inhibitory concentration (IC_{50}) for LAP and NE-LAP were obtained and are shown in Table 2. No differences were found between treatments suggesting that encapsulation did not impair the cytotoxicity of the drug. NE-blank did not impair on cytotoxicity, at all the evaluated concentrations the cell viability was close to 100 %. Therefore, it was not possible to calculate an IC50 value for this

Table 2
Half-maximum inhibitory concentration (IC_{50}) for LAP and NE-LAP against 4T1 and MDA-MB-231 tumor cells ($p < 0.05$).

Treatment	4T1 (μM)	MDA-MB-231 (μM)
LAP	8.29 ± 3.07	6.60 ± 3.1
NE-LAP	10.34 ± 1.06	7.29 ± 1.79

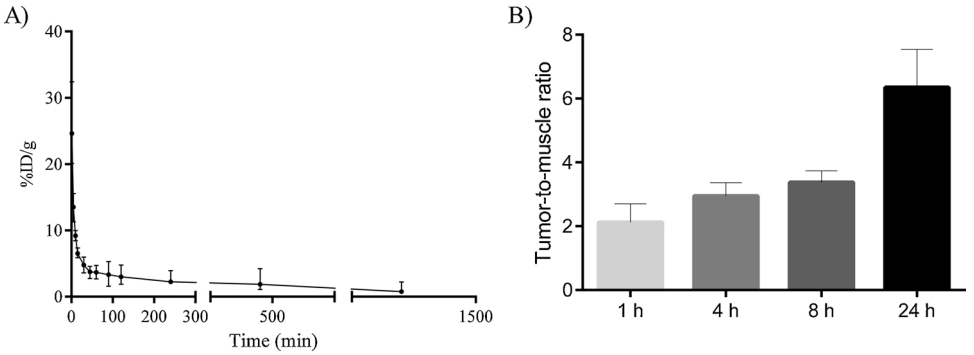

Fig. 7. Blood clearance and the tumor-to-muscle ratio of ^{99m}Tc-NE-LAP. A) Blood circulation of ^{99m}Tc-NE-LAP after intravenous administration in healthy BALC/c female mice. All data are the mean percentage (n = 7) of the injected dose of per gram of blood, ± the standard deviation of the mean. B) Tumor-to-muscle ratio at 1, 4, 8 and 24 h after intravenous administration of ^{99m}Tc-NE-LAP in 4T1 tumor-bearing mice (n = 7).

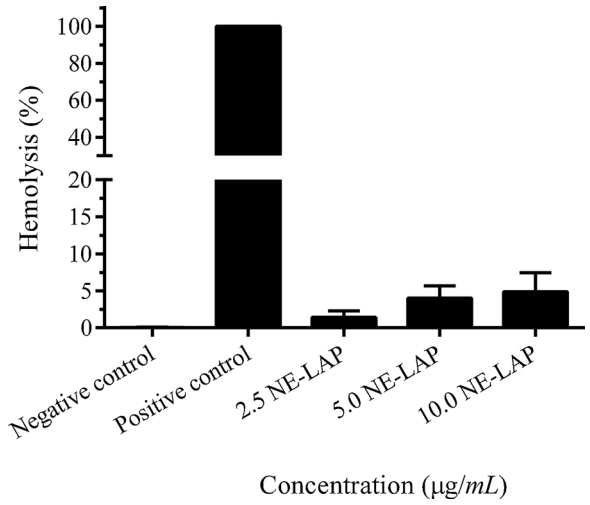

Fig. 8. NE-LAP *in vitro* hemolysis assay. Data are expressed as mean ± sd (n = 5).

group, showing the absence of cytotoxicity of the nanocarrier.

3.8. Hemolysis assay

The hemolytic activity profiles of diff ;erent concentrations of NE-LAP are shown in Fig. 8. It is possible to observe that hemolysis is dose-dependent, reaching a maximum of 4.88 % for NE-LAP at 10 μg/mL (10 NE-LAP). Components with hemolysis values below 10 % can be considered as non-hemolytic [39]. Therefore, NE-LAP proved to be hemocompatible for the intravenous administration.

3.9. Antitumor activity

Fig. 9A shows the 4T1 tumor growth for all the evaluated groups over time. It can be observed that LAP (free and encapsulated) was more effective at controlling tumor growth when compared to the control group. In addition, NE-LAP was statistically different from control and LAP groups, indicating higher efficiency in antitumor activity. Values of RTV and IR (Table 3) corroborate the data found in the tumor growth curve, indicating higher IR and lower RTV for the NE-LAP group.

3.10. Toxicity

Toxicity was evaluated through changes body weight and blood chemistry parameters that assess liver and kidney damage. The body weight was monitored over the treatment, Fig. 9B. It can be noted that the control group had a decrease in weight; meanwhile, the other groups had gained weight. This result indicates that LAP-treated groups showed no signs of potential gut toxicity in this protocol.

Table 4 shows the biochemical analysis of blood from 4T1 tumor-bearing mice treated with free LAP and NE-LAP. Creatinine and urea were performed for kidney function evaluation, while alanine aminotransferase (ALT) and aspartate aminotransferase (AST) were dosed for checking liver function. Comparing to the control group, neither treated groups show any alteration in biochemical parameters, demonstrating a lack of potential dose-limiting organ toxicity. These data were confirmed by histological analysis, since no significant alterations were observed for liver or kidneys slides (Fig. 10).

4. Discussion

Several biological applications have been reported for LAP, including antitumor activity [7,8]. However, its low water solubility, which results in low bioavailability, has limited the use of this drug [9]. In this sense, many strategies to overcome these drawbacks have been applied, such as the use of drug delivery systems [40–45]. The characterization of a new nanosystem is essential for understanding the benefits of the proposed system, as well as the possible toxicities [46]. In this work, we produce a LAP-loaded nanoemulsion stable for 30 days with a

Table 3
Relative tumor volume (RTV) and tumor growth inhibition ratio (IR) after the administration of LAP and NE-LAP.

Group	RTV	IR
Control	6.96	–
LAP	5.51	30.68
NE-LAP	3.22[a,b]	53.71[b]

[a] Represents significant difference as compared with the control group.
[b] Represents significant difference as compared with LAP treatment. *P*-values less than 0.05 were set as the significance level (Tukey's test). The values represent the mean ± SD (n = 7 mice/group).

Table 4
Biochemical parameters of 4T1 tumor-bearing mice after intravenous injection of PBS-Tween 2 % (control group); buffered solution of LAP, and NE-LAP.

	Control	LAP	NE-LAP
Creatinine (mg/dL)	0.35 ± 0.10	0.29 ± 0.04	0.31 ± 0.05
Urea (mg/dL)	19.00 ± 2.00	23.83 ± 3.71	22.67 ± 3.01
ALT (U/L)	25.32 ± 9.88	25.03 ± 5.40	23.72 ± 3.29
AST (U/L)	185.05 ± 51.84	142.75 ± 24.77	139.09 ± 27.92

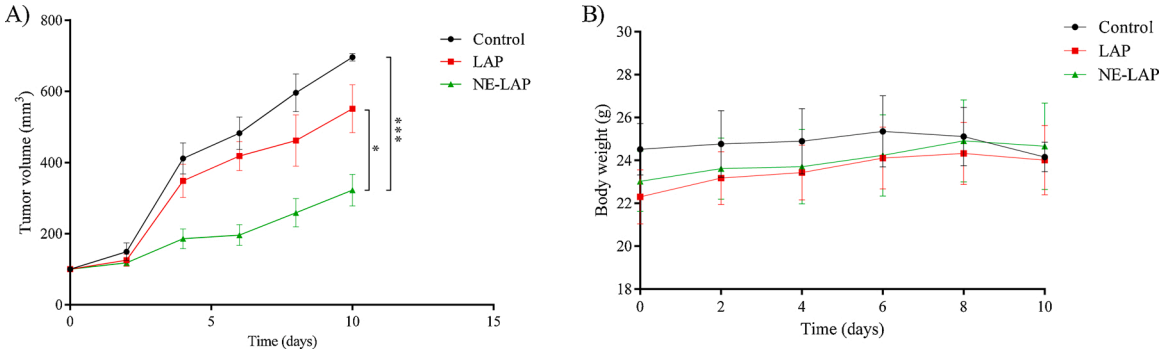

Fig. 9. A) Antitumor effect of PBS-Tween 80 2 % (control), LAP, and NE-LAP on the growth of 4T1 tumor-bearing BALB/c mice. Each treatment was intravenously administered five times, every two days, at a dose of 5 mg/kg/day. Data are expressed by the mean ± standard deviation of the mean. Growth curves were analyzed by one-way ANOVA, followed by Tukey's test. * Represents statistical diff ;erences ($P < 0.05$) between LAP and NE-LAP treatments. *** Represents statistical diff ; erences ($P < 0.001$) between NE-LAP and Control treatments. B) Body weight variation of 4T1 tumor-bearing mice after intravenous injection of PBS-Tween 2 % (control group); buffered solution of LAP, and NE-LAP (* Represents statistical diff ;erences ($P < 0.05$) between the treatments and control group).

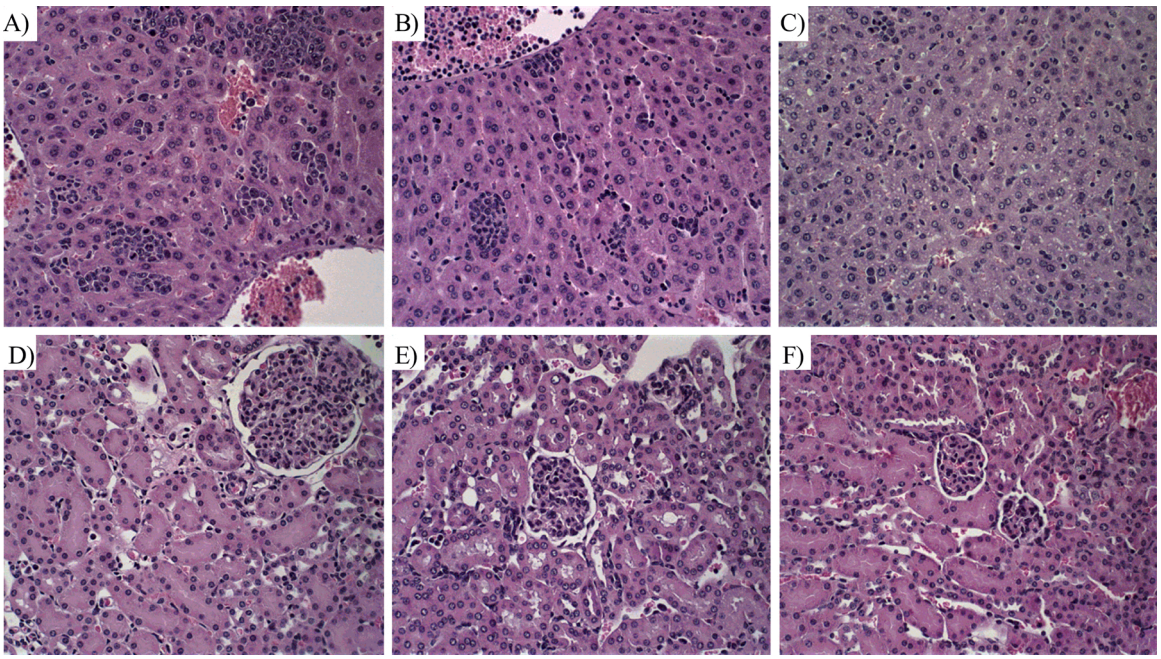

Fig. 10. Histological sections of liver and kidney from breast tumor-bearing female BALB/C mice treated with PBS + 2 %Tween (control), LAP and NE-LAP obtained and stained by Hematoxylin & Eosin. A) Control, liver; B) LAP, liver; C) NE-LAP, liver; D) control, kidney; E) LAP, kidney and F) NE-LAP, kidney. Amplification of 40x.

compatible size, polydispersity index, and zeta potential, in addition to a suitable encapsulation rate for intravenous administration. According to the American Pharmacopoeia, injectable emulsions must have an average diameter of less than 500, with Gaussian distribution, since large particles can get trapped in the lungs, being a risk to the patients [47,48]. It is important to note that the physicochemical characteristics are important parameters for determining the drug's fate in a living organism, providing greater drug concentration in the organ or target of interest to exert its pharmacological action. Rodrigues et al., proposed a submicron emulsion of LAP as a promising delivery platform for natural medicines [19]. Our system differs from this study mainly in the surfactant concentration. The authors have evaluated increasing concentrations of surfactants, reaching an optimum amount of 2.2 %, while we used only 1.5 % in the composition of NE-LAP, with suitable parameters for *in vivo* studies. It is well-known that high concentrations of surfactants might be toxic and should be avoided in intravenous formulations [49,50]. In addition, to the best of our knowledge this is the first report assessing biological behavior and antitumor activity of nanoemulsion of LAP.

A high encapsulation percentage of LAP was achieved and might be related to its increased solubility in the oily phase [51]. However, with the increase of LAP amount into the nanoemulsion, a lack of stability was observed. This may be a result of the saturated system that expels molecules of LAP to the external medium after storage [35,52,53].

NE-LAP radiolabeled studies were carried out to assess the *in vivo* behavior of the system, mainly its capacity of accumulating in the tumor region. It is important to note that the ^{99m}Tc-NE-LAP showed β-half-life more than 2-times longer than free ^{99m}Tc-LAP, which probably contributes to a tumor-to-muscle ratio greater than 2 over time and reaching 6 at 24 h post-injection. Recently, authors have demonstrated the effective nanoparticle tumor accumulation through intracellular pathway preferentially than EPR effect. This fact, along with the already known enhanced permeability of tumor vessels, which is still slightly contributing to tissue accumulation, may represent the reasons for the success of nanoparticles in the anticancer therapy [54]. In both uptake routes, a longer blood circulation time is pivotal since high concentration of the drug is available in the bloodstream, consequently, a high tumor accumulation is achieved.

In sequence, we evaluated if the encapsulation of LAP would impair its cytotoxicity against a murine (4T1) and a human (MDA-MB-231) breast tumor cell lines. It is important to mention that both tumor cells exhibit a triple-negative phenotype, which is considered a very aggressive cancer with poor prognosis and not responsive to classic hormone therapies [55,56]. Cytotoxicity studies reveal an IC_{50} for NE-LAP in the same range of the free drug, indicating the maintenance of antitumor activity even after encapsulation. It is already known that LAP, as a naphthoquinone, might generate reactive oxygen species (ROS) through oxidation by flavoenzymes [57,58]. When the damage caused by ROS is very extensive and the cellular machinery cannot eliminate oxidative stress, the cell goes into apoptosis [59,60].

Further *in vivo* antitumor activity assay confirms the efficacy of NE-LAP in controlling tumor growth. It is important to note that the treatment with NE-LAP leads to a big improvement in the IR when compared to the free drug. This may be related to the improved bioavailability and increased uptake in the tumor region. Similar results were observed by Zhao, (2013) and Han, (2009), where they also obtained better outcomes by encapsulating anticancer drugs in nanoemulsion [61,62]. Additionally, no sign of toxicity was observed in hemolysis assay, biochemical and histological analysis, and body weight, indicating the safety of this treatment.

5. Conclusions

NE-LAP was successfully prepared and characterized showing suitable parameters to support intravenous administration. Short-term stability demonstrated that NE-LAP at 0.5 mg/mL remained stable for 30 days and drug release studies revealed a more sustained release profile. Biodistribution and blood clearance studies confirm an increase in the blood circulation time, which leads to a preferential tumor uptake. These improvements certainly contributed to the higher antitumor activity observed for NE-LAP in contrast to LAP itself. This favorable performance along with the absence of signs of toxicity leads us to indicate NE-LAP as an effective strategy for cancer treatment.

Declaration of Competing Interest

The authors declare they have no conflict of interest.

Acknowledgments

The authors would like to thank Fundação de Amparo à Pesquisa do Estado de Minas Gerais (FAPEMIG-Brazil), Conselho Nacional de Desenvolvimento Científico e tecnológico (CNPq-Brazil) for their financial support and scholarship. The authors also thank the Center of Microscopy from Federal University of Minas Gerais, Brazil, to the assistance in the Cryo-TEM.

References

[1] World Health Organization, The top 10 causes of death. Top 10 Causes Death, 2018, pp. 14–16 (Accessed July 29, 2020), https://www.who.int/news-room/fact-sheets/detail/the-top-10-causes-of-death.
[2] F. Bray, J. Ferlay, I. Soerjomataram, R.L. Siegel, L.A. Torre, A. Jemal, Global cancer statistics 2018: GLOBOCAN estimates of incidence and mortality worldwide for 36 cancers in 185 countries, CA, Cancer J. Clin. 68 (2018) 394–424, https://doi.org/10.3322/caac.21492.
[3] I.J. Fidler, M.L. Kripke, The challenge of targeting metastasis, Cancer Metastasis Rev. 34 (2015) 635–641, https://doi.org/10.1007/s10555-015-9586-9.
[4] Y. Octavia, C.G. Tocchetti, K.L. Gabrielson, S. Janssens, H.J. Crijns, A.L. Moens, Doxorubicin-induced cardiomyopathy: from molecular mechanisms to therapeutic strategies, J. Mol. Cell. Cardiol. 52 (2012) 1213–1225, https://doi.org/10.1016/j.yjmcc.2012.03.006.
[5] R.H. Wijdeven, B. Pang, Y.G. Assaraf, J. Neefjes, Old drugs, novel ways out: drug resistance toward cytotoxic chemotherapeutics, Drug Resist. Updat. 28 (2016) 65–81, https://doi.org/10.1016/j.drup.2016.07.001.
[6] C. Atalay, Multi-drug resistance and cancer, Expert Opin. Ther. Pat. 17 (2007) 511–520, https://doi.org/10.1517/13543776.17.5.511.
[7] K.V. Rao, T.J. Mcbride, J.J. Oleson, Recognition and Evaluation of Lapachol as an Antitumor Agent, Cancer Res. 28 (1968) 1952–1954.
[8] J.B. Block, A.A. Serpick, W. Miller, P.H. Wiernik, Early clinical studies with lapachol (NSC-11905), Cancer Chemother. Rep. 2 (4) (1974) 27–28. http://www.ncbi.nlm.nih.gov/pubmed/4614904.
[9] F. Epifano, S. Genovese, S. Fiorito, V. Mathieu, R. Kiss, Lapachol and its congeners as anticancer agents: a review, Phytochem. Rev. 13 (2014) 37–49, https://doi.org/10.1007/s11101-013-9289-1.
[10] H. Jahangirian, E.G. Lemraski, T.J. Webster, R. Rafiee-Moghaddam, Y. Abdollahi, A review of drug delivery systems based on nanotechnology and green chemistry: Green nanomedicine, Int. J. Nanomedicine 12 (2017) 2957–2978, https://doi.org/10.2147/IJN.S127683.
[11] R. Aboofazeli, Nanometric-scaled emulsions (nanoemulsions), Iran, J. Pharm. Res. 9 (2010) 325–326, https://doi.org/10.22037/ijpr.2010.897.
[12] Y. Singh, J.G. Meher, K. Raval, F.A. Khan, M. Chaurasia, N.K. Jain, M.K. Chourasia, Nanoemulsion: Concepts, development and applications in drug delivery, J. Control. Release 252 (2017) 28–49, https://doi.org/10.1016/j.jconrel.2017.03.008.
[13] T.G. Mason, J.N. Wilking, K. Meleson, C.B. Chang, S.M. Graves, Nanoemulsions: formation, structure, and physical properties, J. Phys. Condens. Matter 18 (2006) R635–R666, https://doi.org/10.1088/0953-8984/18/41/R01.
[14] Marcos Luciano Bruschi, Strategies to Modify the Drug Release from Pharmaceutical Systems, Woodhead Publishing, 2015, https://doi.org/10.1016/B978-0-08-100092-2.00006-0.
[15] L. Chen, B. Chen, L. Deng, B. Gao, Y. Zhang, C. Wu, N. Yu, Q. Zhou, J. Yao, J. Chen, An optimized two-vial formulation lipid nanoemulsion of paclitaxel for targeted delivery to tumor, Int. J. Pharm. 534 (2017) 308–315, https://doi.org/10.1016/j.ijpharm.2017.10.005.
[16] B. Kim, C.D. Pena, D.T. Auguste, Targeted lipid nanoemulsions encapsulating epigenetic drugs exhibit selective cytotoxicity on CDH1-/FOXM1+ Triple Negative breast cancer cells, Mol. Pharm. 16 (2019) 1813–1826, https://doi.org/10.1021/acs.molpharmaceut.8b01065.
[17] M.H. Alkhatib, W.S. Alshehri, F.B. Abdu, In vivo evaluation of the anticancer activity of the gemcitabine and doxorubicin combined in a nanoemulsion, J. Pharm. Bioallied Sci. 10 (2018) 35–42, https://doi.org/10.4103/jpbs.JPBS_225_17.
[18] K. Shanmugapriya, H. Kim, H.W. Kang, In vitro antitumor potential of astaxanthin nanoemulsion against cancer cells via mitochondrial mediated apoptosis, Int. J. Pharm. 560 (2019) 334–346, https://doi.org/10.1016/j.ijpharm.2019.02.015.
[19] F.V.S. Rodrigues, L.S. Diniz, R.M.G. Sousa, T.D. Honorato, D.O. Simão, C.R. M. Araújo, T.M. Gonçalves, L.A. Rolim, P.L. Goto, A.C. Tedescoc, M.P. Siqueira-Moura, Preparation and characterization of nanoemulsion containing a natural naphthoquinone, Quim. Nova 41 (2018) 756–761, https://doi.org/10.21577/0100-4042.20170247.
[20] D.P. De Santana, S.G.C. Fonseca, D.C.G. Bedor, L.B. Leal, J.A. Silva, Aplicação termoanalítica no desenvolvimento e caracterização de micropartículas de PLGA contendo lapachol, Rev. Ciencias Farm. Basica e Apl. 29 (2008) 261–266 (Accessed July 29, 2020), http://serv-bib.fcfar.unesp.br/seer/index.php/Cien_Farm/article/viewFile/593/516.
[21] M.A.M. Tabosa, A.R.B. de Andrade, A.A.M. Lira, V.H.V. Sarmento, D.P. de Santana, L.B. Leal, Microemulsion Formulations for the Transdermal Delivery of Lapachol, AAPS PharmSciTech 19 (2018) 1837–1846, https://doi.org/10.1208/s12249-018-0995-2.
[22] A.A.M. Lira, E.D.A. Sester, L.R.P. Abreu, L.B.L. Da Silva, A.G. Wanderley, D.P. De Santana, Desenvolvimento preliminar de gel de lapachol: Estudo de permeação in vitro, Rev. Bras. Ciencias Farm. J. Pharm. Sci. 40 (2004) 35–41, https://doi.org/10.1590/S1516-93322004000100007.
[23] A.A.M. Lira, E.A. Sester, A.L.M. Carvalho, R.R. Strattmann, M.M. Albuquerque, A. G. Wanderley, D.P. Santana, Development of lapachol topical formulation: Anti-inflammatory study of a selected formulation, AAPS PharmSciTech 9 (2008) 163–168, https://doi.org/10.1208/s12249-007-9002-z.
[24] S.G.C. Fonseca, L.B.L. Da Silva, R.F. Castro, D.P. De Santana, Validation of the analytical methodology for evaluation of lapachol in solution by HPLC, Quim. Nova 27 (2004) 157–159, https://doi.org/10.1590/S0100-40422004000100026.
[25] D.W. Malcolm, J.J. Varghese, J.E. Sorrells, C.E. Ovitt, D.S.W. Benoit, The effects of biological fluids on colloidal stability and siRNA delivery of a pH-Responsive micellar nanoparticle delivery system, ACS Nano 12 (2018) 187–197, https://doi.org/10.1021/acsnano.7b05528.
[26] R.S. Fernandes, J. De Oliveira Silva, S.C.A. Lopes, S. Chondrogiannis, D. Rubello, V. N. Cardoso, M.C. Oliveira, L.A.M. Ferreira, A.L.B. De Barros, Technetium-99m-labeled doxorubicin as an imaging probe for murine breast tumor (4T1 cell line) identification, Nucl. Med. Commun. 37 (2016) 307–312, https://doi.org/10.1097/MNM.0000000000000443.
[27] S.E. Miranda, J.A. Lemos, R.S. Fernandes, F.M. Ottoni, R.J. Alves, A. Ferretti, D. Rubello, V.N. Cardoso, A.L. Branco de Barros, Technetium-99m-labeled lapachol as an imaging probe for breast tumor identification, Rev. Esp. Med. Nucl. Imagen Mol. 38 (2019) 167–172, https://doi.org/10.1016/j.remn.2018.10.006.
[28] V. Vichai, K. Kirtikara, Sulforhodamine B colorimetric assay for cytotoxicity screening, Nat. Protoc. 1 (2006) 1112–1116, https://doi.org/10.1038/nprot.2006.179+.
[29] E.A. Leite, C.M. Souza, A.D. Carvalho-Júnior, L.G.V. Coelho, A.M.Q. Lana, G. D. Cassali, M.C. Oliveira, Encapsulation of cisplatin in long-circulating and pH-sensitive liposomes improves its antitumor effect and reduces acute toxicity, Int. J. Nanomedicine 7 (2012) 5259–5269, https://doi.org/10.2147/IJN.S34652.
[30] D.C. Litzinger, A.M.J. Buiting, N. van Rooijen, L. Huang, Effect of liposome size on the circulation time and intraorgan distribution of amphipathic poly(ethylene glycol)-containing liposomes, BBA - Biomembr. 1190 (1994) 99–107, https://doi.org/10.1016/0005-2736(94)90038-8.
[31] R.A. Petros, J.M. Desimone, Strategies in the design of nanoparticles for therapeutic applications, Nat. Rev. Drug Discov. 9 (2010) 615–627, https://doi.org/10.1038/nrd2591.
[32] D. Liu, D.T. Auguste, Cancer targeted therapeutics: From molecules to drug delivery vehicles, J. Control. Release 219 (2015) 632–643, https://doi.org/10.1016/j.jconrel.2015.08.041.
[33] S.S. Davis, Pharmaceutical aspects of intravenous fat emulsions, Eur. J. Hosp. Pharm. Sci. Pract. (September) (1974) 165–171.
[34] J. Brouwers, M.E. Brewster, P. Augustijns, Supersaturating drug delivery systems: the answer to solubility-limited oral bioavailability? J. Pharm. Sci. 98 (2009) 2549–2572, https://doi.org/10.1002/jps.21650.
[35] Y. Li, J. Zheng, H. Xiao, D.J. McClements, Nanoemulsion-based delivery systems for poorly water-soluble bioactive compounds: Influence of formulation parameters on polymethoxyflavone crystallization, Food Hydrocoll. 27 (2012) 517–528, https://doi.org/10.1016/j.foodhyd.2011.08.017.
[36] D.B. Warren, H. Benameur, C.J.H. Porter, C.W. Pouton, Using polymeric precipitation inhibitors to improve the absorption of poorly water-soluble drugs: a mechanistic basis for utility, J. Drug Target. 18 (2010) 704–731, https://doi.org/10.3109/1061186X.2010.525652.
[37] F. Bruxel, M. Laux, L.B. Wild, M. Fraga, L.S. Koester, H.F. Teixeira, Nanoemulsões como sistemas de liberação parenteral de fármacos, Quim. Nova 35 (2012) 1827–1840, https://doi.org/10.1590/S0100-40422012000900023.
[38] T.U.S.P. Convention, The United States Pharmacopeia: USP 41: The National Formulary: NF 36, 34th ed., Rockville, Md.The United States Pharmacopeial Convention, Rockville, 2018.
[39] K. Amin, R.-M. Dannenfelser, In vitro hemolysis: guidance for the pharmaceutical scientist, J. Pharm. Sci. 95 (2006) 1173–1176, https://doi.org/10.1002/jps.20627.
[40] A. Esteves-Souza, K.A. Lucio, A.S. Da Cunha, A. Da Cunha Pinto, E.L. Da Silva Lima, C.A. Camara, M.D. Vargas, C.R. Gattass, Antitumoral activity of new polyamine-naphthoquinone conjugates, Oncol. Rep. 20 (2008) 225–231. http://www.ncbi.nlm.nih.gov/pubmed/18575741.
[41] K.O. Eyong, P.S. Kumar, V. Kuete, G.N. Folefoc, E.A. Nkengfack, S. Baskaran, Semisynthesis and antitumoral activity of 2-acetylfuranonaphthoquinone and other naphthoquinone derivatives from lapachol, Bioorganic Med. Chem. Lett. 18 (2008) 5387–5390, https://doi.org/10.1016/j.bmcl.2008.09.053.
[42] M.C.F. da Linardi, M.M. de Oliveira, M.R.P. Sampaio, A Lapachol Derivative Active against Mouse Lymphocytic Leukemia P-388, J. Med. Chem. 18 (1975) 1159–1161, https://doi.org/10.1021/jm00245a027.
[43] W. Kandioller, E. Balsano, S.M. Meier, U. Jungwirth, S. Göschl, A. Roller, M. A. Jakupec, W. Berger, B.K. Keppler, C.G. Hartinger, Organometallic anticancer complexes of lapachol: Metal centre-dependent formation of reactive oxygen species and correlation with cytotoxicity, Chem. Commun. 49 (2013) 3348–3350, https://doi.org/10.1039/c3cc40432c.
[44] A. Ventura Pinto, S. Lisboa de Castro, The trypanocidal activity of naphthoquinones: a review, Molecules 14 (2009) 4570–4590, https://doi.org/10.3390/molecules14114570.

[45] C. Zhang, Y. Qu, B. Niu, Design, synthesis and biological evaluation of lapachol derivatives possessing indole scaffolds as topoisomerase I inhibitors, Bioorg. Med. Chem. Lett. 24 (2016) 5781–5786, https://doi.org/10.1016/j.bmc.2016.09.034.
[46] A.J. Trevor, B.G. Katzung, M. Knuidering-Hall, Cancer chemotherapy. Katzung Trevor's Pharmacol. Exam. Board Rev., 12th ed., McGraw-Hill Medical Publishing (Ed.), 2012.
[47] D.F. Driscoll, Lipid Injectable Emulsions: Pharmacopeial and Safety Issues, Pharm. Res. 23 (2006) 1959–1969, https://doi.org/10.1007/s11095-006-9092-4.
[48] T.U.S.P. Convention, GLOBULE Size Distribution in Lipid Injectable Emulsions - USP32-NF27, 2012, pp. 2011–2013.
[49] B. Arechabala, C. Coiffard, P. Rivalland, L.J.M. Coiffard, Y. De Roeck-Holtzhauer, Comparison of cytotoxicity of various surfactants tested on normal human fibroblast cultures using the neutral red test, MTT assay and LDH release, J. Appl. Toxicol. 19 (1999) 163–165, https://doi.org/10.1002/(SICI)1099-1263(199905/06)19:3<163::AID-JAT561>3.0.CO;2-H.
[50] R.K. Varma, R. Kaushal, A.Y. Junnarkar, G.P. Thomas, M.U. Naidu, P.P. Singh, R. M. Tripathi, D.R. Shridhar, Polysorbate 80: a pharmacological study, Arzneimittelforschung 35 (1985) 804–808. http://www.ncbi.nlm.nih.gov/pubmed/4026903.
[51] C.Y. Lui, A.A. Ayeni, C. Gyllenhaal, M.J. Groves, Some formulation properties of lapachol, a potential oncolytic agent of natural origin, Drug Dev. Ind. Pharm. 11 (1985) 1763–1779, https://doi.org/10.3109/03639048509057698.
[52] C.M.R. Oda, R.S. Fernandes, S.C. de Araújo Lopes, M.C. de Oliveira, V.N. Cardoso, D.M. Santos, A.M. de Castro Pimenta, A. Malachias, R. Paniago, D.M. Townsend, P. M. Colletti, D. Rubello, R.J. Alves, A.L.B. de Barros, E.A. Leite, Synthesis, characterization and radiolabeling of polymeric nano-micelles as a platform for tumor delivering, Biomed. Pharmacother. 89 (2017) 268–275, https://doi.org/10.1016/j.biopha.2017.01.144.
[53] G.W. Aherne, A. Hardcastle, F. Raynaud, A.L. Jackman, Immunoreactive dUMP and TTP pools as an index of thymidylate synthase inhibition; effect of tomudex (ZD1694) and a nonpolyglutamated quinazoline antifolate (CB30900) in L1210 mouse leukaemia cells, Biochem. Pharmacol. 51 (1996) 1293–1301, https://doi.org/10.1016/0006-2952(96)00035-4.
[54] S. Sindhwani, A.M. Syed, J. Ngai, B.R. Kingston, L. Maiorino, J. Rothschild, P. MacMillan, Y. Zhang, N.U. Rajesh, T. Hoang, J.L.Y. Wu, S. Wilhelm, A. Zilman, S. Gadde, A. Sulaiman, B. Ouyang, Z. Lin, L. Wang, M. Egeblad, W.C.W. Chan, The entry of nanoparticles into solid tumours, Nat. Mater. 19 (2020) 566–575, https://doi.org/10.1038/s41563-019-0566-2.
[55] K.J. Chavez, S.V. Garimella, S. Lipkowitz, Triple negative breast cancer cell lines: one tool in the search for better treatment of triple negative breast cancer, Breast Dis. 32 (2010) 35–48, https://doi.org/10.3233/BD-2010-0307.
[56] P. Kau, G.M. Nagaraja, H. Zheng, D. Gizachew, M. Galukande, S. Krishnan, A. Asea, A mouse model for triple-negative breast cancer tumor-initiating cells (TNBC-TICs) exhibits similar aggressive phenotype to the human disease, BMC Cancer 12 (2012), https://doi.org/10.1186/1471-2407-12-120.
[57] M.O.F. Goulart, P. Falkowski, T. Ossowski, A. Liwo, Electrochemical study of oxygen interaction with lapachol and its radical anions, Bioelectrochemistry 59 (2003) 85–87, https://doi.org/10.1016/S1567-5394(03)00005-7.
[58] Z. Darzynkiewicz, E. Bedner, F. Traganos, Difficulties and pitfalls in analysis of apoptosis, Methods Cell Biol. 63 (2001) 527–546, https://doi.org/10.1016/s0091-679x(01)63028-0.
[59] H. Lecoeur, M.C. Prévost, M.L. Gougeon, Oncosis is associated with exposure of phosphatidylserine residues on the outside layer of the plasma membrane: A reconsideration of the specificity of the annexin V/propidium iodide assay, Cytometry 44 (2001) 65–72, https://doi.org/10.1002/1097-0320(20010501)44:1<65::AID-CYTO1083>3.0.CO;2-Q.
[60] H. Lecoeur, M.T. Melki, H. Saïdi, M.L. Gougeon, Chapter three analysis of apoptotic pathways by multiparametric flow cytometry: application to HIV infection, Methods Enzymol. 442 (2008) 51–82, https://doi.org/10.1016/S0076-6879(08)01403-1.
[61] H. Zhao, H. Lu, T. Gong, Z. Zhang, Nanoemulsion loaded with lycobetaine-oleic acid ionic complex: Physicochemical characteristics, in vitro, in vivo evaluation, and antitumor activity, Int. J. Nanomedicine 8 (2013) 1959–1973, https://doi.org/10.2147/IJN.S43892.
[62] M. Han, C.X. He, Q.L. Fang, X.C. Yang, Y.Y. Diao, D.H. Xu, Q.J. He, Y.Z. Hu, W. Q. Liang, B. Yang, J.Q. Gao, A novel camptothecin derivative incorporated in nano-carrier induced distinguished improvement in solubility, stability and anti-tumor activity both in vitro and in vivo, Pharm. Res. 26 (2009) 926–935, https://doi.org/10.1007/s11095-008-9795-9.